Food Chemistry 119 (2010) 154–160

Contents lists available at ScienceDirect

Food Chemistry

journal homepage: www.elsevier.com/locate/foodchem

Characterisation of 2-Cys peroxiredoxin isozyme (Prx1) from *Taiwanofungus camphorata* (Niu-chang-chih): Expression and enzyme properties

Yi-Jen Liau [a,1], Yu-Ting Chen [b,1], Choa-Yi Lin [c,1], Jenq-Kuen Huang [d,1], Chi-Tsai Lin [a,*]

[a] Institute of Bioscience and Biotechnology and Center for Marine Bioscience and Biotechnology, National Taiwan Ocean University, Keelung 202, Taiwan
[b] Institute of Bioinformatics, National Chung Hsing University, Taichung 402, Taiwan
[c] Graduate Institute of Medical Sciences, Taipei Medical University, Taipei 110, Taiwan
[d] Department of Chemistry, Western Illinois University, 1 University Circle, Macomb, IL 61455-1390, USA

ARTICLE INFO

Article history:
Received 16 December 2008
Received in revised form 1 May 2009
Accepted 8 June 2009

Keywords:
Taiwanofungus camphorata
Three-dimensional homology structure (3-D homology structure)
2-Cys peroxiredoxin isozyme (Prx1)

ABSTRACT

Peroxiredoxins (Prxs) are a family of antioxidant peroxidases. The functions of Prxs comprises of cell protection against oxidative stress and regulation of cell proliferation. A putative 2-Cys Prx isozyme (Prx1) cDNA was cloned from *Taiwanofungus camphorata* (commonly known as Niu-chang-chih in Taiwan). The deduced amino acid sequence is conserved amongst the reported Prxs. A 3-D homology structure was created for this Prx1. To characterise the *T. camphorata* Prx1, the coding region was subcloned into a pAVD10 and transformed into *Escherichia coli*. The recombinant 6His-tagged Prx1 was expressed and purified by Ni^{2+}-nitrilotriacetic acid sepharose. The purified enzyme showed two forms using a 15% SDS–PAGE. The enzyme retained 60% activity at 60 °C for 2.5 min. The enzyme was stable under a broad pH range from 5 to 11. The enzyme showed 57% activity after 40 min of incubation at 37 °C with trypsin. The ability of the enzyme to protect intact supercoiled plasmid DNA from $^{\cdot}OH$ induced nicking was demonstrated.

1. Introduction

Peroxiredoxins (Prxs) constitute a group of peroxidases found in a wide variety of organisms (Rhee, Kang et al., 2005). The enzymes play important roles in antioxidation (Neumann et al., 2003). They perform the protective antioxidant roles by reducing hydrogen peroxide and alkyl hydroperoxides using thiols as reductants (Bryk, Griffin, & Nathan, 2000). Prxs use the redox-active peroxidatic cysteine (C_P) located at the N-terminal portion of the molecule to reduce peroxides (Wood, SchrÖder, Harris, & Poole, 2003). During the peroxidase reaction, the C_P residue in the active site is oxidised to sulfenic acid (C_P–SOH), whereas hydrogen peroxide and alkyl hydroperoxides are reduced to water, or the corresponding alcohol (Ellis & Poole, 1997a, 1997b). Prxs are classified into two types, 1-Cys or 2-Cys, based on whether they contain one or two conserved Cys residues (Chon, Choi, Kim, & Shin, 2005; Manevich, Feinstein, & Fisher, 2004). The 2-Cys Prxs contain a second conserved resolving Cys (C_R) residue at the C-terminal portion of the molecule. The 2-Cys Prxs have been further subdivided into either typical or atypical types depending on the location of the C_R residue. In typical 2-Cys Prxs, the C_P–SOH reacts with the C_R–SH residue located in the C-terminal portion of the second subunit of the enzyme homodimer to form an intermolecular disulphide (Chae, Uhm, & Rhee, 1994). In atypical 2-Cys Prxs, the C_P–SOH reacts with the C_R–SH residue within the same subunit forming an intramolecular disulphide. The disulphide is then reduced by thioredoxin, or glutathione (Dietz, 2003) completing the catalytic cycle.

Several *in vitro* and *in vivo* studies have implicated the potential roles of 2-Cys Prxs as either therapeutic targets or diagnostic biomarkers for major diseases such as the suppression of Prx II (belonging to a 2-Cys Prx) expression using antisense cDNA has been demonstrated to render cancer cells more susceptible to radiation-induced apoptosis (Park et al., 2000). Prx I (belonging to a 2-Cys Prx) expression is elevated in most cancers, and the possibility that recombinant 2-Cys Prx proteins could be useful for cancer prevention cannot be excluded (Kang, Rhee, Chang, Jeong, & Choi, 2005). Similarly, recombinant Prx I and Prx II exhibit antiviral activity, inhibiting HIV-1 replication (Geiben-Lynn et al., 2003).

Taiwanofungus camphorata (formerly named *Antrodia camphorata,* commonly known as Niu-chang-chih in Taiwan) is a unique mushroom species found only in the forests of Taiwan which uses *Cinnamomum kanehirai* hay as its host. The fruiting bodies of *T. camphorata* have been used in herbal medicine for many years. *T. camphorata* has been shown to exhibit an antioxidative (Hsiao et al., 2003) and anti-inflammatory (Shen et al., 2004) response, amongst others. This encouraged us to search for active components in *T. camphorata*. Recently, we have cloned and characterised a phospholipid hydroperoxide glutathione peroxidase (Chen, Lin,

* Corresponding author. Tel.: +886 2 24622192x5513; fax: +886 2 24622320.
E-mail address: B0220@mail.ntou.edu.tw (C.-T. Lin).
[1] Contributed equally to this work.

0308-8146/$ - see front matter © 2009 Elsevier Ltd. All rights reserved.
doi:10.1016/j.foodchem.2009.06.008

Ken, Wen, & Lin, 2009), a glutathione-dependent formaldehyde dehydrogenase (Huang, Ken, Wen, & Lin, 2009), a catalase (Ken, Chen, Chang, & Lin, 2008), a 1-Cys Prx (Wen, Huang, Juang, & Lin, 2007), a cambialistic-superoxide dismutase (Liau, Wen, Shaw, & Lin, 2007) and a 2-Cys Prx (called Prx in Fig. 1). We also clone this 2-Cys Prx isozyme (called Prx1 in Fig. 1) different sequence in C-terminal from Prx (shown in Fig. 1). The Prx enzymes may be one of the important physiological components in *T. camphorata*. It may be possible that the *T. camphorata* Prx1 reported here is one of the ingredients responsible for increasing human anti-inflammation (Mitsui et al., 2002). Understanding the properties of this Prx1 would be of interest due to its importance. Thus, the coding region of the *T. camphorata* Prx1 cDNA was introduced into an *Escherichia coli* expression system, the active enzyme was purified and its properties studied. Here, we report the cloning and characterisation of an antioxidant enzyme, Prx1, from *T. camphorata*.

2. Materials and methods

2.1. RNA extraction from T. camphorata and cDNA synthesis

Fruiting bodies of *T. camphorata* which was naturally grown in the hay of *C. kanehirai* were obtained from central part of Taiwan. Total RNA was prepared from fresh fruiting bodies (wet weight 1.3 g) using TRIzol reagent (GIBCO, Frederick, Maryland) as described before (Ken, Hsiung, Huang, Juang, & Lin, 2005). The total RNA (4.2 μg) was obtained. Three micrograms of the total RNA were used for cDNA synthesis using a ZAP-cDNA kit from Stratagene (La Jolla, California).

2.2. Isolation of Prx1 cDNA

We have previously established an expressed sequence tag (EST) database from fruiting bodies of *T. camphorata* and sequenced all clones with insert size greater than 0.4 kb (data not shown). The identity of a Prx1 cDNA clone was assigned by comparing the inferred amino acid sequence in various databases using the basic local alignment search tool BLAST (http://www.ncbi.nlm.nih.gov/blast/Blast.cgi).

2.3. Bioinformatic analysis

The BLAST program was used to search homologous protein sequences in the nonredundant database (NRDB) at the National Center for Biotechnology Information, National Institutes of Health (http://www.ncbi.nlm.nih.gov/). Multiple alignments were constructed using ClustalW2 program (http://www.ebi.ac.uk/Tools/clustalw2/index.html). Structural modelling was carried out using the SWISS-MODEL program (http://swissmodel.expasy.org/SWISS-MODEL.html) to create a three-dimensional (3-D) homology structure based on the known X-ray structure of human peroxiredoxin 4 (PDB code 2pn8_E) as template. The modelling data was then superimposed by DeepView Swiss-PdbViewer v3.7 (http://www.expasy.org/spdbv/) using human thioredoxin peroxidase-B (PDB code 1qmv_H) from red blood cells as a template to obtain a better structure alignment (Schröder et al., 2000).

2.4. Subcloning Prx1 cDNA to an expression vector

The coding region of the Prx1 cDNA was amplified using two gene-specific primers. The 5′ upstream primer contains an *Nde*I recognition site (5′ GGA ATT CCA TAT GGT CGC CAT CGT CCA GAA 3′) and the 3′ downstream primer contains 6His-tagged and *Hind*III recognition site (5′ CCC AAG CTT CTA GTG GTG GTG GTG GTG GTC AAC GCG AGC ACG CTT CTT G 3′). Using 0.1 μg of *T. camphorata* cDNA as a template, and 10 pmol of each 5′ upstream and 3′ downstream primers, a 0.7 kb fragment was amplified by PCR. The fragment was ligated into pCR2.1 and transformed into *E. coli* TOPO10 for further sequence analysis. Plas-

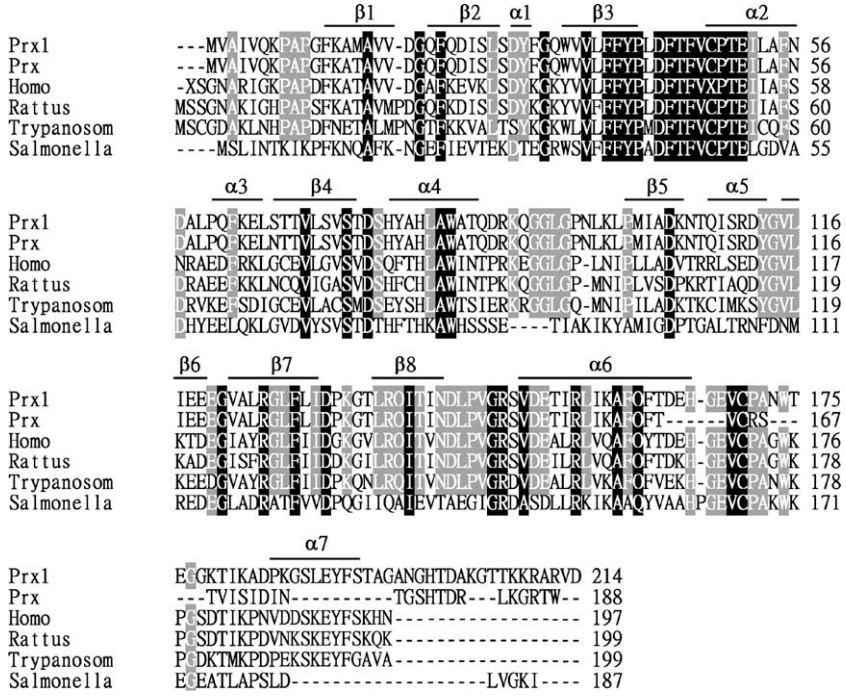

Fig. 1. Optimal alignment of the amino acid sequences of Prxs and homology structure prediction. Sequence alignment: Prx1 (this study, accession no. AY383653), Prx (*T. camphorata*, accession no. AY450599), Rattus (*Rattus norvegicus*, accession no. Q63716), Homo (*Homo sapiens*, PDB code 1qmv_H), Trypanosoma (*Trypanosoma cruzi*, accession no. O96763), and Salmonella (*Salmonella typhimurium*, accession no. P0A251). Identical amino acids in all sequences are shaded black, conservative replacements are shaded grey. Protein secondary structure was predicted by SWISS-MODEL program and represented as α helices and β strands.

mid DNA was isolated from the clone and digested with *Nde*I and *Hind*III. The digestion products were separated on a 0.8% agarose gel. The 0.7 kb insert DNA was gel purified and subcloned into *Nde*I and *Hind*III sites of pAVD 10 vector (Avidis, France). The recombinant DNA was then transformed into *E. coli* C43(DE3).

2.5. Expression and purification of the recombinant Prx1

The transformed *E. coli* containing the Prx1 was grown at 37 °C in 200 ml of Luria Bertani (LB) medium containing 50 μg/ml ampicillin until A_{600} reached 0.9. Protein expression was induced by addition of isopropyl β-D-thiogalactopyranoside (IPTG) to a final concentration of 1 mM. The culture was incubated for an additional 4 h with shaking at 150 rpm, and then the bacterial cells were harvested by centrifugation. Cells were suspended in 2 ml of PBS containing 1% glycerol and 1 g glass beads to break bacterial cells mechanically. The content was vortexed for 5 min and centrifuged at 10,000*g* for 5 min. The extraction procedure was repeated three times, and the supernatants were combined. The final crude extract (12 ml) was loaded on a Ni-nitrilotriacetic acid sepharose (Qiagen) column (with 2 ml bed volume). The column was washed with 12 ml of PBS containing 5 mM imidazole. The enzyme was eluted with 6 ml of PBS containing 100 mM imidazole (at a flow rate of 0.4 ml/min and 1.5 ml/fraction at room temperate). The purified enzyme (3 ml) was dialysed against 200 ml of 0.03× PBS containing 0.5% glycerol at 4 °C for 4 h. Fresh 0.03× PBS containing 0.5% glycerol was changed once during dialysis as described before (Ken et al., 2005). The dialysed sample was either used directly for analysis or stored at −20 °C until use. Protein concentration was determined by a Bio-Rad Protein Assay Kit (Richmond, CA) using bovine serum albumin as a standard.

2.6. Prx1 activity assay (ferrithiocyanate assay)

The recombinant Prx1 (0.8 μg protein) was incubated in 45–47 μl buffer (1 mM DTT/0.03× PBS/0.5% glycerol) for 2 min at room temperature. The reaction was initiated by addition of 3–5 μl of 1 mM H_2O_2. At 0 and 10 min reaction times, 20 μl of 26% trichloroacetic acid was added to the 50 μl reaction mixture to stop the reaction. The peroxidase activity was determined by following the disappearance of the peroxide substrate (the total peroxide, 3–5 nmol at the beginning of the reaction minus the remaining amount at the end of 10 min). The remaining peroxide content was determined as a red-coloured ferrithiocyanate complex formed by addition 20 μl of 10 mM $Fe(II)(NH_4)(SO_4)_2$ and 10 μl of 2.5 M KSCN to the 70 μl of reaction mixture. The colour was quantified by absorbance measurement at 475 nm (Thurman, Ley, & Scholz, 1972).

2.7. Enzyme characterisation

To test the stability of Prx1 under various conditions. Aliquots of the recombinant Prx1 sample (2.5 μg) were used to study the following: (a) *Thermal effect*. Enzyme sample was heated at 60 °C for 2, 4, 8 or 16 min. (b) *pH effect*. Enzyme sample was adjusted to desired pH by adding a half volume of buffer with different pH values: 0.2 M citrate buffer (pH 2.0 or 5.0), 0.2 M Tris–HCl buffer (pH 8.0 or 9.0) or 0.2 M glycine–NaOH buffer (pH 10.0 or 11.0). Each sample was incubated at 37 °C for 30 min. (c) *SDS effect*. SDS, a protein denaturing reagent, was added to the enzyme sample to the final concentration of 0.5, 1, or 2% (v/v) and then incubated at 37 °C for 30 min. (d) *Imidazole effect*. During protein purification, the Prx1 enzyme was eluted with imidazole. Therefore, the effect of imidazole on enzyme activity was examined. Imidazole was added to the enzyme sample to final concentrations of 0.1, 0.2, or 0.4 M and incubated at 37 °C for 30 min. (e) *Susceptibility to digestive proteases*. The enzyme was incubated with one-tenth its weight of trypsin or chymotrypsin at pH 8.0, 37 °C for a period of 10, 20 or 40 min. In the chymotrypsin digestion, $CaCl_2$ was added to a final concentration of 5 mM. After each treatment, 1.5 μg of each treated sample was electrophoresed onto a 15% native gel to determine changes in protein levels. The other 0.8 μg of each treated sample was used for ferrithiocyanate assay.

2.8. Thiol mixed-function oxidation (MFO) assay

The Prx1-dependent inactivation of DNA cleavage was evaluated by a thiol mixed-function oxidation assay (Kawazu et al., 2001). Reaction mixture (15 μl) containing 40 μM $FeCl_3$, 10 mM DTT, 25 mM HEPES (pH 7.0) and 750 ng of pUC19 plasmid DNA was incubated with or without the Prx1 protein (310 or 465 ng) at 25 °C for 1 or 2 h. After incubation, nicking of the supercoiled plasmids was evaluated on 1% agarose gels stained with ethidium bromide.

3. Results

3.1. Cloning and characterisation of a cDNA encoding Prx1

Approximately 20,000 *T. camphorata* cDNA clones were sequenced. Nucleotide sequences and the inferred amino acid sequences of these clones were compared to the sequences in various nucleic acid and protein data banks using the appropriate BLAST programs (http://www.ncbi.nlm.nih.gov/blast/Blast.cgi). A putative Prx1 cDNA clone was identified by sequence homology to published Prxs (Chon et al., 2005). The Prx1 cDNA (942 bp, EMBL accession no. AY383653) encodes a protein of 214 amino acid residues with a calculated molecular mass of 23,552 Da. Fig. 1 shows the amino acid sequence alignment of the putative Prx1 with Prx from several sources. This Prx1 shared 75% identity with Prx from *T. camphorata* (accession no. AY450599), 54% and 55% identity with Prx from Rattus (*Rattus norvegicus*, Q63716) and Homo (*Homo sapiens*, 1qmv_H), and 48% and 51% with Prx from Trypanosom (*Trypanosoma cruzi*, O96763) and Salmonella (*Salmonella typhimurium*, P0A251). The active site residues around C_P, the F-motif (FTFVCPTEI), and the hydrophobic region around C_R (VCPXXW) are highly conserved as seen in other published 2-Cys Prxs (KÖnig et al., 2003).

3.2. Expression and purification of the recombinant Prx1

The coding region of Prx1 was amplified by PCR and subcloned into an expression vector, pAVD 10 as described in the Section 2. Positive clones were verified by DNA sequence analysis. The recombinant Prx1 protein was expressed, and the proteins were analysed using a 15% SDS–PAGE after heat denaturation in the presence a reducing agent (Fig. 2A). The recombinant Prx1 was expressed as a 6His-tagged fusion protein and was purified by affinity chromatography with nickel chelating sepharose. A band with molecular mass of about 23 kDa (expected size of Prx1 monomer) was detected in Ni–NTA eluted fractions by SDS–PAGE (Fig. 2A, lanes 4–9). The purified protein was also analysed by SDS–PAGE under non-reducing condition. In the absence of DTT, the Prx1 was visible as a major band with molecular size corresponding to its dimer and a minor band corresponding to the monomer (Fig. 2B, lane 1). The major bands represent two forms of the dimers with a double or single disulphide linkage between Cys48 and Cys170. A reductive dissociation of the dimeric Prx1 was seen when the protein was incubated with DTT (Fig. 2B, lane 2). The monomer appeared as the major band. The Ni–NTA eluted fractions containing pure protein were pooled and characterised fur-

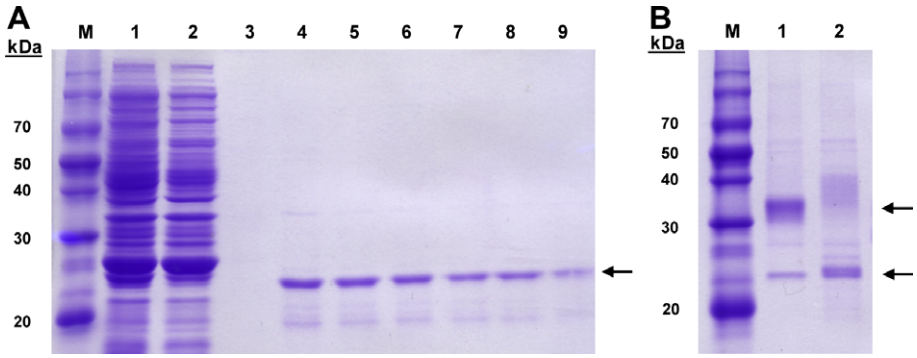

Fig. 2. Coomassie blue-stained SDS–polyacrylamide gel showing the purification of 6His-tagged Prx1 expressed in *E. coli*. Fifteen microlitre (loading buffer with mercaptoethanol and boiling 5 min) of each fraction was loaded into each lane of the 15% SDS–PAGE. (A) Lane 1, crude extract from *E. coli* expressing Prx1; 2, flow-through proteins from the Ni–NTA column; 3, wash; lanes 4–9, purified Prx1 eluted from Ni–NTA column fractions 1–6. (B) Lane 1, purified Prx1 (1.5 μg protein) after dialysis in 0.03× PBS containing 0.5% glycerol (absence DTT); purified Prx1 (1.5 μg protein) treated with 1 mM DTT for 10 min. Sample (loading buffer without mercaptoethanol and without boiling) was loaded into each lane of the 15% SDS–PAGE. Molecular masses (in kDa) of standards are shown at left. Arrows denote dimer and monomer.

ther. The yield of the purified 6His-tagged Prx1 was 50 μg from 200 ml of culture. Functional Prx1 was detected by the activity assay as describe below.

3.3. Antioxidant activity of the Prx1

The ability of the Prx1 to remove H_2O_2 was evaluated using the ferrithiocyanate system. This Prx1 showed the ability to remove H_2O_2 without supplementing thiols. Such activity was promoted more efficiently if DTT was added at 1 mM (Fig. 3A). The result indicates that DTT is capable of reducing the oxidised form of the Prx1 to regenerate its activity. This Prx1 catalysed the removal of H_2O_2 in the presence of DTT in a concentration-dependent manner (Fig. 3A). This Prx1's ability to remove H_2O_2 was not supported by the presence of 1 mM GSH (Fig. 3A). In the present study, we showed that the Prx1 can use DTT, an artificial reductant, *in vitro*. Although our results showed that GSH is not an effective reductant *in vitro*, its ability to serve as electron donors *in vivo* for reduction of peroxides remains to be investigated. It has been reported that GSH can serve as an electron donor *in vitro* for Prx VI (1-Cys Prx) when πGST is present (Manevich et al., 2004). The representative time-course study under the substrate (H_2O_2) concentration of 250 μM was shown in Fig. 3B. The Trx (thioredoxin)-linked peroxidase activity of the Prx1 was tested by monitoring the oxidation of

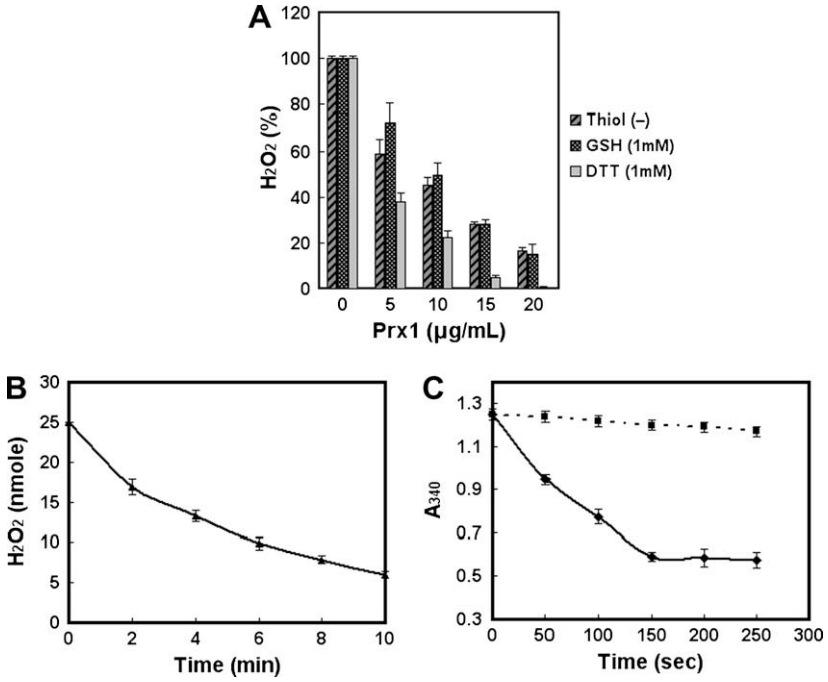

Fig. 3. Peroxidase activity of Prx1. The effect of 1 mM DTT or 1 mM GSH (A) on the activity of Prx1 to remove H_2O_2 was examined in a 50 μl reaction volume. Various concentrations of the Prx1 protein were incubated with H_2O_2 (60 μM) in the presence or absence of thiols for 10 min. The remaining H_2O_2 in the reaction mixture was measured using the ferrithiocyanate system. The results were expressed as the percentage of H_2O_2 recorded with the Prx1 relative to that recorded without the Prx1. Data are the means of three experiments. (B) Time-dependent removal of H_2O_2 (25 nmol) by the Prx1 protein (20 μg/ml) with 1 mM DTT was recorded from 2 to 10 min in a 50 μl reaction volume. The reactions were stopped at 2 min intervals. The remaining H_2O_2 in the reaction mixture was measured using the ferrithiocyanate system. The results were expressed as 1 nmol of H_2O_2 calculated on the basis of A_{475} recorded at the indicated time. Data are means of three independent experiments. (C) NADPH oxidation coupled by the Prx1 (solid line) to reduction of H_2O_2 in the presence of *E. coli* Trx and Trx R system. NADPH oxidation was monitored as the decrease in A_{340} in a 100 μl reaction mixture (0.2 μM TR, 8 μM Trx, 0.25 mM NADPH, 50 μg/ml Prx1 protein, 100 μM H_2O_2, 0.03× PBS and 0.5% glycerol). The dotted line was in the absence of Prx1. Data are means of three experiments.

NADPH in the presence of *E. coli* Trx/Trx R (thioredoxin reductase) system (Fig. 3C). After the addition of H_2O_2, the system showed a decrease in A_{340}, in the presence of the Prx1 due to the oxidation of NADPH. The result suggests that the Prx1 can be characterised as a thioredoxin peroxidase.

3.4. Characterisation of the purified Prx1

To examine the thermal effect of the enzyme activity, the purified Prx1 was heat-treated as described in the Section 2 and then analysed using 15% native gel or activity assay. The activity appeared to be somewhat heat stable. Approximately 40% of the Prx1 activity was lost at 60 °C for 2.5 min (Fig. 4A and B). The Prx1 activity had no effect in a broad range of pH from 5 to 11 as shown in Fig. 4C. The enzyme retained 40.5% activity in 2% SDS (Fig. 4D). This enzyme retained about 45% activity in 0.2 M imidazole (Fig. 4E). The enzyme showed 46% activity after 20 min of incubation at 37 °C with one-tenth its weight of chymotrypsin (Fig. 4F). This enzyme showed 57.1% activity after 40 min of incubation at 37 °C with trypsin (data not shown). The Prx1 protein as shown in Fig. 1 contains 17 potential trypsin cleavage sites and 18 potential chymotrypsin-high specificity (C-term to [FYW], not before P) cleavage sites. However, the enzyme appeared to be susceptible to chymotrypsin (Fig. 4F) but resistant to digestion by trypsin even at a high enzyme/substrate (w/w) ratio of 1/10 (data not shown).

To test the peroxidase activity of the Prx1, we used the assay of plasmid DNA protection against ROS generated by the Fenton reaction induced by the metal-catalysed system. In the presence of Prx1, the alteration of the plasmid DNA from the supercoiled to the nicked form was prevented. The inhibition was dose-dependent (Fig. 5). The assay employs a system that generates hydroxyl radicals to damage DNA. In the absence of Prx1 enzyme, the hydroxyl radicals produced in the system caused nicking of the DNA, as evidenced by a shift in gel mobility of the supercoiled plasmid. The addition of purified Prx1 enzyme to the MFO system at a mass of 310 and 465 ng prevented nicking of the supercoiled DNA, demonstrating the antioxidant activity of Prx1.

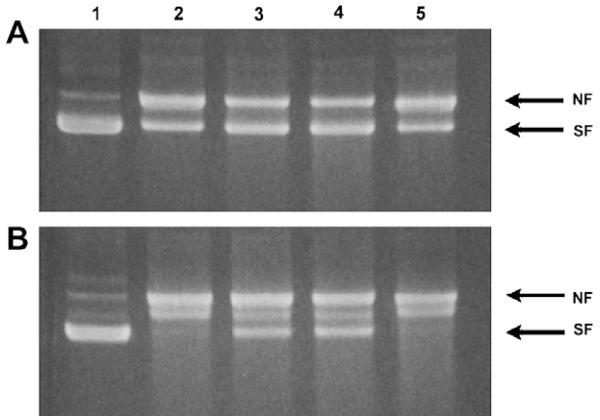

Fig. 5. Functional activity of recombinant Prx1. The reaction was performed in a mixture consisting of 40 μM $FeCl_3$, 10 mM DTT, 25 mM HEPES (pH 7.0) and 750 ng of pUC19 plasmid DNA. The reaction was stopped after incubation for 1 h (A), 2 h (B) and the plasmid DNA was analysed on ethidium bromide stained agarose gel. Lane 1, only DNA; 2, DNA + Fe^{3+} + DTT; 3, DNA + Fe^{3+} + DTT + 310 ng Prx1; 4, DNA + Fe^{3+} + DTT + 465 ng Prx1; 5, DNA + Fe^{3+} + DTT + 465 ng BSA. SF, supercoiled form; NF, nicked form.

4. Discussion

According to Chon et al. classification (Chon et al., 2005), typical 2-Cys Prxs are defined by the pattern "P .{6} C_P .{60, 90} R .{40, 50} C_R". This expression is translated as: (Pro)-(6 any residues)-(Cys)-(between 60 and 90 of any residues)-(Arg)-(between 40 and 50 of any residues)-(Cys). Atypical 2-Cys Prxs R type are defined by the pattern "P .{6} C_P .{60, 90} R .{20, 25} C_R". This expression is translated as: (Pro)-(6 any residues)-(Cys)-(between 60 and 90 of any residues)-(Arg)-(between 20 and 25 of any residues)-(Cys). This Prx1 has the pattern: (Pro at the position 41)-(6 residues)-(Cys at the position 48)-(76 residues)-(Arg at the position 125)-(44 residues)-(Cys at the position 170). Our other Prx (shown in

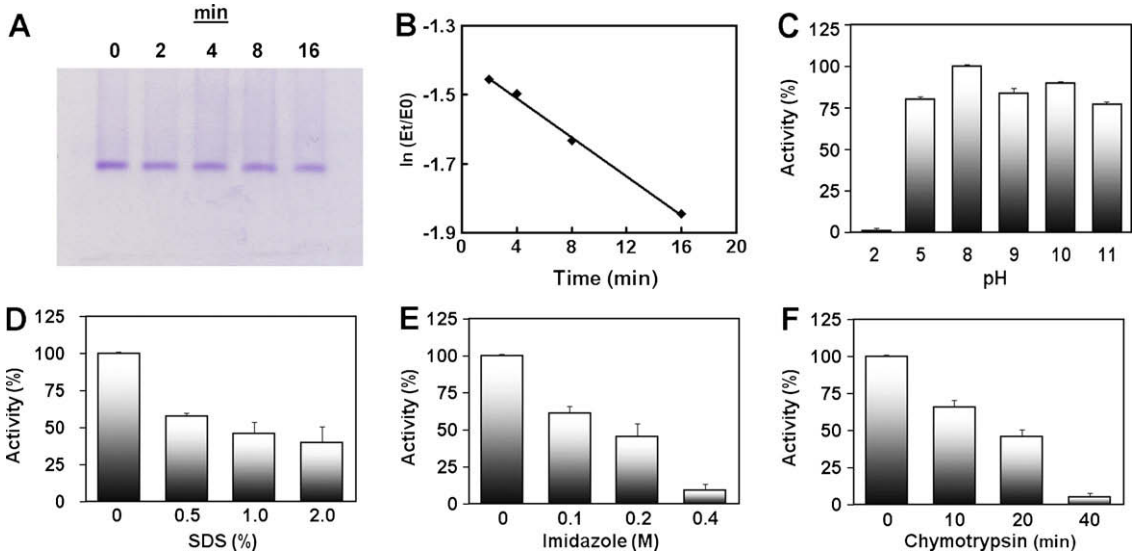

Fig. 4. Effect of temperature, pH, SDS, imidazole and chymotrypsin on the purified Prx1. The enzyme sample was heated at 60 °C for various time intervals. Aliquots of the sample were taken at 0, 2, 4, 8 or 16 min and analysed by 15% native-PAGE or assayed for enzyme activity. (A) Staining for protein (1.5 μg protein per lane) after separation on a 15% native-PAGE. (B) Plot of thermal inactivation kinetics. Prx1 activity assay (0.8 μg protein/time interval). E_0 and E_t are original activity and residual activity after being heated for different time intervals. (C) The enzyme samples were incubated with a different pH buffer at 37 °C for 30 min and then assayed for Prx1 activity (0.8 μg protein/pH point). (D) The enzyme samples were incubated with various concentrations of SDS at 37 °C for 30 min and then checked for activity (0.8 μg protein/SDS level). (E) The enzyme samples were incubated with various concentrations of imidazole at 37 °C for 30 min and then checked for Prx1 activity (0.8 μg protein/imidazole level). (F) The enzyme samples were incubated with chymotrypsin at 37 °C for various time and then checked for Prx1 activity (0.8 μg protein/time interval). Data are means of three independent experiments.

Fig. 1) has the pattern: (Pro at the position 41)-(6 residues)-(Cys at the position 48)-(76 residues)-(Arg at the position 125)-(39 residues)-(Cys at the position 165). However, in *T. camphorata* Prx1, Arg125 and Cys170 are separated by 44 residues, whereas in *T. camphorata* Prx, Arg125 and Cys165 is separated by 39 residues instead of typical 2-Cys Prxs where R and C_R are separated by between 40 and 50 of any residues. In addition, the two disulphide-forming Cys residues of typical 2-Cys Prxs are separated by 120–123 amino acids, whereas those of the atypical are separated by <104 residues (Rhee, Kang, Chang, Jeong, & Kim, 2001; Rhee, Yang, Kang, Woo, & Chang, 2005). This Prx1 is separated by 122 residues matched typical 2-Cys Prxs, whereas the other *T. camphorata* Prx is separated by 117 residues not matched both typical and atypical.

A structural model of Prx1 was created based on the known X-ray structure of human peroxiredoxin 4 (2pn8_E) and was superimposed by using human thioredoxin peroxidase-B (1qmv_H) as a template to obtain a better structure alignment (Fig. 6) *via* SWISS-MODEL and DeepView Swiss-PdbViewer v3.7 programs. The amino acid sequences of Prx1 and the human peroxiredoxin 4 share 61% homology. The secondary structure was predicted by the same program and represented as α helices and β strands (Fig. 1). Structure studies of Prx (Wood, Poole, & Karplus, 2003; Wood, SchrÖder et al., 2003) have showed that (a) the C_P is surrounded by three residues conserved in all Prx classes – Pro41, Thr45 and Arg125 (this Prx1 numbering). The Pro41 limits peroxide access to C_P and shields C_P sulfenic acid from further oxidation by peroxides. The Thr45 might position the proton for abstraction by an unidentified catalytic base, and the Arg125 might aid this by stabilizing the growing negative charge on the sulphur. The presence of Pro41, Thr45 and Arg125 surrounding the C_p in this Prx1 confirm the identity of the clone. (b) Phosphorylation of mammalian typical Prx at the conserved residue Thr89 (this Prx1 numbering is 85) by cyclin-dependent kinases was to decrease the peroxidase activity. The presence of a similar phosphorylation site in this Prx1 suggests that phosphorylation may be a common regulatory mechanism amongst Prxs. (c) Two features uniquely present in all the Prxs are the three residue insertion associated with a conserved Gly91-Gly-Leu-Gly94 sequence (this Prx1 no.) and the addition helix present as a C-terminal extension associated with a conserved Tyr-Phe sequence (YF motif). The YF motif of C-terminal helix was reported to serve as a keystone that stabilizes the whole region of the structure (Wood, Poole et al., 2003). This Prx1 possesses both GGLG and YF motif. It is interesting to note that *T. camphorata* Prx (shown in Fig. 1) only possesses GGLG but lacks YF motif. This discrepancy suggests that this Prx1 is typical 2-Cys Prx.

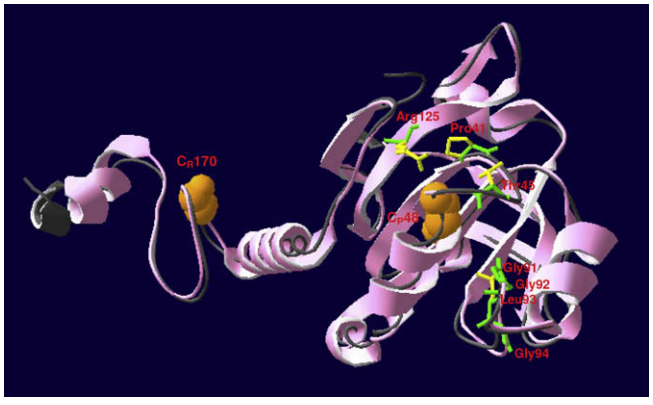

Fig. 6. 3-D homology structure of Prx1. The structural model of Prx1 was created based on the known X-ray structure of human peroxiredoxin 4 (2pn8_E) and was superimposed by using human thioredoxin peroxidase-B (1qmv_H) as a template to obtain a better structure alignment *via* SWISS-MODEL and DeepView Swiss-PdbViewer v3.7 programs. Superimposition of Prx1 (pink) and human thioredoxin peroxidase-B (grey) was shown by using protein solid ribbons. The five residues (Pro41, Thr45, Cys48, Arg125, and Cys170) are conserved as they are present in all reported 2-Cys Prx sequences.

Like all 2-Cys Prxs, the *T. camphorata* Prx1 has the highly conserved active site around C_P, the F-motif (FTFVCPTEI), and the hydrophobic region around C_R (VCPXXW) (KÖnig et al., 2003). The F-motif of *T. camphorata* Prx matches the Prx1, but the hydrophobic around C_R (VCRXXV) shows a two-residue difference compared to *T. camphorata* Prx1. Taken together all of the above sequence analysis, this Prx1 is a typical 2-Cys Prxs. The sequence difference between the two *T. camphorata* Prx1 and Prx at the C-terminal region may have arisen from alternative pre-mRNA splicing.

As shown in Fig. 6, from the point of the structure that Cys48 and Cys170 are far apart enough and are not expected to form intramolecular disulphide bond. Therefore, we assume that the Prx1 favours formation of dimers through intermolecular disulphide linkages. This assumption is supported by our SDS–PAGE analysis of the purified protein in the presence or absence of DTT. In the absence of DTT, the dimeric form is predominant (see Fig. 2B, lane 1). The dimers may be linked by two disulphide bonds between Cys48–Cys170 and Cys170–Cys48, or between Cys48–Cys48 and Cys170–Cys170. The dimers may also be linked by one disulphide bond between Cys48 and Cys170, or Cys48–Cys48, or Cys170–Cys170 (Chae et al., 1994). The Prx1 shows smeared dimeric bands between 35 and 40 kDa, reflecting the presence of various dimeric forms. For instance, the dimer with two disulphide bonds should be more compact, therefore moved faster than the dimers with only one disulphide bond on SDS–PAGE (Fig. 2B). It has been reported that 2-Cys Prx from the human malaria parasite *Plasmodium falciparum* (Kawazu et al., 2000) only exists in two forms (monomer and dimer) similar to this Prx1. We did not observe hexadecameric formation in this Prx1 as that found in *Aeropyrum pernix* K1 (Jeon & Ishikawa, 2003). Factors reported to promote oligomerisation of typical 2-Cys Prxs include high or low ionic strength, low pH, high magnesium or calcium concentrations, reduction of the redox-active disulphide center, and over oxidation of the C_P to a sulfinic acid (Wood, SchrÖder et al., 2003). It remains to be studied that this Prx1 may form oligomers under some of the above mentioned conditions.

We are particularly interested in the antioxidant effects of *T. camphorata.* As a step towards understanding the antioxidant effects, we cloned the antioxidant enzyme Prx1 from *T. camphorata* expressed in *E. coli* and characterised it. The enzyme was characterised in terms of the thermal stability of the enzyme activity, the influence by pH, SDS, imidazole or proteases sensitivity. Heat stability and imidazole effects were tested because the information is useful for developing enzyme purification protocols. Protease tests were useful in understanding the effect of the digestive enzymes to the Prx1 and its suitability as a health food. The Prx1 appears to be active in a broad range of pH's from 5 to 11 (Fig. 4C). This result suggested that the active site residue Cp (Cys48) can catalyse the peroxidase reaction whether its in the protonated form (low pH) or in the thiolate form (high pH). This phenomena is in agreement with that reported by Wood, SchrÖder et al. (2003).

This enzyme appears to be stable under various conditions. These properties may be beneficial for its potential medical applications including removal of peroxide in wounded tissue to promote healing or serve as health foods.

Acknowledgement

This work was supported by the National Science Council of the Republic of China under Grant NSC 97-2313-B-019-001-MY3 to C-T. L.

References

Bryk, R., Griffin, P., & Nathan, C. (2000). Peroxynitrite reductase activity of bacterial peroxiredoxins. *Nature, 407*, 211–215.

Chae, H. Z., Uhm, T. B., & Rhee, S. G. (1994). Dimerization of thiol-specific antioxidant and the essential role of cysteine 47. *Proceedings of the National Academy of Sciences of the United States of America, 1*, 7022–7026.

Chen, H. T., Lin, C. Y., Ken, C. F., Wen, L., & Lin, C. T. (2009). Putative phospholipid hydroperoxide glutathione peroxidase from *Antrodia camphorata*. *Food Chemistry, 115*, 476–482.

Chon, J. K., Choi, J., Kim, S. S., & Shin, W. (2005). Classification of peroxiredoxin subfamilies using regular expressions. *Genomics and Informatics, 3*, 55–60.

Dietz, K. J. (2003). Plant peroxiredoxins. *Annual Review of Plant Biology, 54*, 93–107.

Ellis, H. R., & Poole, L. B. (1997a). Novel application of 7-chloro-4-nitrobenzo-2-oxa-1,3-diazole to identify cysteine sulfenic acid in the AhpC component of alkyl hydroperoxide reductase. *Biochemistry, 36*, 15013–15018.

Ellis, H. R., & Poole, L. B. (1997b). Roles for the two cysteine residues of AhpC in catalysis of peroxide reduction by alkyl hydroperoxide reductase from *Salmonella typhimurium*. *Biochemistry, 36*, 13349–13356.

Geiben-Lynn, R., Kursar, M., Brown, N. V., Addo, M. M., Shau, H., Lieberman, J., et al. (2003). HIV-1 antiviral activity of recombinant natural killer cell enhancing factors, NKEF-A and NKEF-B, members of the peroxiredoxin family. *Journal of Biological Chemistry, 278*, 1569–1574.

Hsiao, G., Shen, M. Y., Lin, K. H., Lan, M. H., Wu, L. Y., Chou, D. S., et al. (2003). Antioxidative and hepatoprotective effects of *Antrodia camphorata* extract. *Journal of Agricultural and Food Chemistry, 51*, 3302–3308.

Huang, C. Y., Ken, C. F., Wen, L., & Lin, C. T. (2009). An enzyme possessing both glutathione-dependent formaldehyde dehydrogenase and S-nitrosoglutathione reductase from *Antrodia camphorata*. *Food Chemistry, 112*, 795–802.

Jeon, S. J., & Ishikawa, K. (2003). Characterization of novel hexadecameric thioredoxin peroxidase from *Aeropyrum pernix* K1. *Journal of Biological Chemistry, 278*, 24174–24180.

Kang, S. W., Rhee, S. G., Chang, T. S., Jeong, W., & Choi, M. H. (2005). 2-Cys peroxiredoxin function in intracellular signal transduction: Therapeutic implications. *Trends in Molecular Medicine, 11*, 571–578.

Kawazu, S. I., Komaki, K., Tsuji, N., Kawai, S., Ikenoue, N., Hatabu, T., et al. (2001). Molecular characterization of a 2-Cys peroxiredoxin from the human malaria parasite *Plasmodium faciparum*. *Molecular and Biochemical Parasitology, 116*, 73–79.

Kawazu, S. I., Tsuji, N., Hatabu, T., Kawai, S., Matsumoto, Y., & Kano, S. (2000). Molecular cloning and characterization of a peroxiredoxin from the human malaria parasite *Plasmodium falciparum*. *Molecular and Biochemical Parasitology, 109*, 165–169.

Ken, C. F., Chen, H. T., Chang, R. C., & Lin, C. T. (2008). Biochemical characterization of a catalase from *Antrodia camphorata*: Expression in *Escherichia coli* and enzyme properties. *Botanical Studies, 49*, 119–125.

Ken, C. F., Hsiung, T. M., Huang, Z. X., Juang, R. H., & Lin, C. T. (2005). Characterization of Fe/Mn-superoxide dismutase from diatom *Thallassiosira weissflogii*: Cloning, expression, and property. *Journal of Agricultural and Food Chemistry, 53*, 1470–1474.

KÖnig, J., Lotte, K., Plessow, R., Brockhinke, A., Baier, M., & Dietz, K. J. (2003). Reaction mechanism of plant 2-Cys peroxiredoxin. *Journal of Biological Chemistry, 278*, 24409–24420.

Liau, Y. J., Wen, L., Shaw, J. F., & Lin, C. T. (2007). A highly stable cambialistic-superoxide dismutase from *Antrodia camphorata*: Expression in yeast and enzyme properties. *Journal of Biotechnology, 131*, 84–91.

Manevich, Y., Feinstein, S. I., & Fisher, A. B. (2004). Activation of the antioxidant enzyme 1-CYS peroxiredoxin requires glutathionylation mediated by heterodimerization with πGST. *Proceedings of the National Academy of the Sciences of the United States of America, 101*, 3780–3785.

Mitsui, A., Hamuro, J., Nakamura, H., Kondo, N., Hirabayashi, Y., Ishizaki-Koizumi, S., et al. (2002). Overexpression of human thioredoxin in transgenic mice controls oxidative stress and life span. *Antioxidants and Redox Signaling, 4*, 693–696.

Neumann, C. A., Krause, D. S., Carman, C. V., Das, S., Dubey, D. P., Abraham, J. L., et al. (2003). Essential role for the peroxiredoxin Prdx1 in erythrocyte antioxidant defence and tumour suppression. *Nature, 424*, 561–565.

Park, S. H., Chung, Y. M., Lee, Y. S., Kim, H. J., Kim, J. S., Chae, H. Z., et al. (2000). Antisense of human peroxiredoxin II enhances radiation-induced cell death. *Clinical Cancer Research, 6*, 4915–4920.

Rhee, S. G., Kang, S. W., Chang, T. S., Jeong, W., & Kim, K. (2001). Peroxiredoxin, a novel family of peroxidases. *IUBMB Life, 52*, 35–41.

Rhee, S. G., Kang, S. W., Jeong, W., Chang, T. S., Yang, K. S., & Woo, H. A. (2005). Intracellar messenger function of hydrogen peroxide and its regulation by peroxiredoxins. *Current Opinion in Cell Biology, 17*, 183–189.

Rhee, S. G., Yang, K. S., Kang, S. W., Woo, H. A., & Chang, T. S. (2005). Controlled elimination of intracellular H_2O_2: Regulation of peroxiredoxin, catalase, and glutathione peroxidase via post-translational modification. *Antioxidants and Redox Signaling, 7*, 619–626.

Schröder, E., Littlechild, J. A., Lebedev, A. A., Errington, N., Vagin, A. A., & Isupov, M. N. (2000). Crystal structure of decameric 2-Cys peroxiredoxin from human erythrocytes at 1.7 Å resolution. *Structure, 8*, 605–615.

Shen, Y. C., Chou, C. J., Wang, Y. H., Chen, C. F., Chou, Y. C., & Lu, M. K. (2004). Anti-inflammatory activity of the extracts from mycelia of *Antrodia camphorata* cultured with water-soluble fractions from five different *Cinnamomum* species. *FEMS Microbiology Letters, 231*, 137–143.

Thurman, R. G., Ley, H. G., & Scholz, R. (1972). Hepatic microsomal ethanol oxidation. Hydrogen peroxide formation and the role of catalase. *European Journal of Biochemistry, 25*, 420–430.

Wen, L., Huang, H. M., Juang, R. H., & Lin, C. T. (2007). Biochemical characterization of 1-Cys peroxiredoxin from *Antrodia camphorata*. *Applied Microbiology and Biotechnology, 73*, 1314–1322.

Wood, Z. A., Poole, L. B., & Karplus, P. A. (2003). Peroxiredoxin evolution and the regulation of hydrogen peroxide signaling. *Science, 300*, 650–653.

Wood, Z. A., SchrÖder, E., Harris, J. R., & Poole, L. B. (2003). Structure, mechanism and regulation of peroxiredoxins. *Trends in Biochemical Sciences, 28*, 32–40.